HHS Public Access

Author manuscript

Oncogene. Author manuscript; available in PMC 2016 January 22.

Published in final edited form as:

Oncogene. 2015 May 14; 34(20): 2609–2620. doi:10.1038/onc.2014.200.

EFNA3 long noncoding RNAs induced by hypoxia promote metastatic dissemination

L Gómez-Maldonado[1,9], **M Tiana**[1,9], **O Roche**[1,2], **A Prado-Cabrero**[1,10], **L Jensen**[3,4], **A Fernandez-Barral**[1], **I Guijarro-Muñoz**[5], **E Favaro**[6], **G Moreno-Bueno**[1], **L Sanz**[5], **J Aragones**[7], **A Harris**[6], **O Volpert**[8], **B Jimenez**[1], and **L del Peso**[1,2]

[1]Departamento de Bioquímica, Universidad Autónoma de Madrid (UAM) and Instituto de Investigaciones Biomédicas 'Alberto Sols' (CSIC-UAM), Madrid, Spain

[2]IdiPaz, Instituto de Investigación Sanitaria del Hospital Universitario La Paz, Madrid, Spain

[3]Department of Medicine and Health Sciences, Linköping University Linköping, Sweden

[4]Department of Microbiology, Tumor and Cell Biology, Karolinska Institute, Stockholm, Sweden

[5]Molecular Immunology Unit, Hospital Universitario Puerta de Hierro Majadahonda, Madrid, Spain

[6]Molecular Oncology Laboratories, Weatherall Institute of Molecular Medicine, University of Oxford, John Radcliffe Hospital, Oxford, UK

[7]Research Unit, Hospital Universitario Santa Cristina, Research Institute Princesa, Autonomous University of Madrid, Madrid, Spain

[8]Urology Department, Northwestern University Feinberg School of Medicine, Chicago, IL, USA

Abstract

The presence of hypoxic regions in solid tumors is an adverse prognostic factor for patient outcome. Here, we show that hypoxia induces the expression of Ephrin-A3 through a novel hypoxia-inducible factor (HIF)-mediated mechanism. In response to hypoxia, the coding *EFNA3* mRNA levels remained relatively stable, but HIFs drove the expression of previously unknown long noncoding (Inc) RNAs from *EFNA3* locus and these IncRNA caused Ephrin-A3 protein accumulation. Ephrins are cell surface proteins that regulate diverse biological processes by modulating cellular adhesion and repulsion. Mounting evidence implicates deregulated ephrin function in multiple aspects of tumor biology. We demonstrate that sustained expression of both Ephrin-A3 and novel *EFNA3* lncRNAs increased the metastatic potential of human breast cancer cells, possibly by increasing the ability of tumor cells to extravasate from the blood vessels into surrounding tissue. In agreement, we found a strong correlation between high *EFNA3* expression and shorter metastasis-free survival in breast cancer patients. Taken together, our results suggest

Correspondence: Dr L del Peso, Department of Biochemistry, Instituto de Investigaciones Biomédicas, 'Alberto sols' Universidad Autonoma de Madrid, Facultad de Medicina, CSIC-UAM, Arturo Duperier, 4, Madrid 28029, Spain. luis.peso@uam.es.

[9]These authors contributed equally to this work.

[10]Current address: King Abdullah University of Science and Technology, Thuwal, Saudi Arabia.

CONFLICT OF INTEREST

The authors declare no conflict of interest.

Supplementary Information accompanies this paper on the Oncogene website (http://www.nature.com/onc)

that hypoxia could contribute to metastatic spread of breast cancer via HIF-mediated induction of *EFNA3* lncRNAs and subsequent Ephrin-A3 protein accumulation.

INTRODUCTION

In a variety of pathologic situations, oxygen demand exceeds its supply to affected tissues leading to a condition known as hypoxia. In particular, hypoxia is frequently observed in solid tumors and, importantly, it has been suggested to be an adverse prognostic factor for patient outcome.[1,2]

At the cellular level, oxygen homeostasis is largely dependent on the induction of a specific gene expression program under the control of the hypoxia-inducible factors (HIFs). HIFs are heterodimers composed of α- and β-subunits that belong to the basic helix–loop–helix Per-ARNT-Sim family.[3] In mammals, three genes encode HIFα subunits, *HIF1A*, *EPAS1/HIF2A* and *HIF3A*, of which HIF-1α and *EPAS1* are the best characterized.[4] Oxygen regulates the stability [5,6] and transcriptional activity[7–9] of HIFα without affecting HIFβ function. The induction of the HIF transcriptional program results in cellular adaptation to hypoxia, a response that aims to restore oxygen supply to hypoxic regions through the induction of erythropoiesis and angiogenesis and to reduce oxygen consumption by reprogramming cellular metabolism.

HIFs role in cancer has been extensively investigated. On the one hand, as hypoxia develops in tumors due to the rapid expansion of the transformed cells, HIF is activated contributing to critical aspects of tumor progression.[1,10] On the other hand, von Hippel-Lindau (VHL) tumor suppressor, which has a key role in the control of HIFα stability,[11–13] is frequently lost in clear-cell renal cell carcinomas (ccRCC). Moreover, several lines of evidence point to HIFs, in particular *EPAS1*, as an ethiologic factor in this kind of cancer.[14] Other oncogenes and tumor suppressor genes including *PTEN*, *mTORC1*, *Ras*, *Akt* and *p53* also regulate the HIF activity.[15] Importantly, the correlation between tumor hypoxia and/or HIFα expression with poor prognosis and increased risk of metastasis has been repeatedly demonstrated in diverse tumor types.[2] Not surprisingly, many of the HIF target genes are involved in biologic processes that impact the metastatic spread of cancer cells, such as angiogenesis, epithelial–mesenchymal transition, cell motility, intra/extravasation and control of the premetastatic niche.[16]

Ephrins are a large family of cell surface ligands that mediate intercellular adhesion and repulsion through interaction with a large group of receptor tyrosine kinases, the Eph receptors.[17,18] Ephrins play essential roles during development, where they guide migration and positioning of the cells for proper tissue patterning. Their function has been particularly well characterized in the nervous system, where Ephrins/Eph function as axon guidance molecules, and in the cardiovascular system, where they control vasculogenesis and angiogenesis.[17] Ephrins are separated into two families according to their structure. Type A Ephrins (Ephrin-A1 to -A5) are glycosylphosphatidyl-inositol-linked membrane-bound ligands, whereas type B ephrins (Ephrin-B1 to -B3) contain a single transmembrane domain and a short cytoplasmic tail.[19] Interestingly, many of the biologic functions of ephrins and Ephs are co-opted by transformed cells and contribute to tumor progression.[20] Accordingly,

many ephrin family members are altered in human cancers and their expression often correlates with a more aggressive phenotype, invasion, metastasis and poor prognosis.[21] In addition to their role in adhesion and repulsion, Eph/Ephrins may contribute to tumor progression and metastasis by altering angiogenesis.[21] Intriguingly, HIF-dependent regulation of Ephrin-A1, Ephrin-B2, EphA2 and EphA4 has been described in a mouse model of skin hypoxia,[22] suggesting a potential link between intratumoral hypoxia, ephrin/Eph expression and tumor progression. In agreement, Ephrin-A1 is upregulated at the transcription level, via *EPAS1*, in hypoxic tumors and this upregulation contributes to increased tumor vascularization.[23,24] Altogether, these works suggest a link between tumoral hypoxia and progression to aggressive phenotype via HIF-mediated regulation of Ephrin expression.

In this study, we show that hypoxia leads to Ephrin-A3 protein accumulation via a previously unknown mechanism that involves HIF-mediated transcriptional upregulation of a novel group of lncRNAs encoded by the *EFNA3* locus. Using animal models and *in vitro* assays, we demonstrate that Ephrin-A3 expression leads to metastatic spread. In contrast with previous studies, we observed no effect on vascularization, but a strong repulsive action, which leads to increased intra- and extravasation that underlies the promotion of metastatic spread by *EFNA3*. Finally, the analysis of public gene expression profiling data sets revealed that *EFNA3* is induced by HIF in human tumors and this induction is predictive of poor prognosis and increased risk of metastasis.

RESULTS

EFNA3 locus encodes lncRNAs that are regulated by hypoxia

We first identified *EFNA3*, a member of the ephrin type A ligands, as the potential novel HIF target gene using an *in silico* search.[25] As a first step to validate this prediction, we determined the level of Ephrin-A3 protein and found that it was induced by hypoxia in several cell lines (Figure 1a). The Ephrin-A3 species we detected had an apparent molecular weight of approximately 72 kDa, much higher than the 26.3 kDa molecular weight predicted from its amino-acid sequence, owing to posttranslational modifications (Supplementary Figure 1). Next, we decided to study the effect of hypoxia on *EFNA3* mRNA. According to curated databases (RefSeq), the *EFNA3* locus encodes for a single mRNA isoform (NM_004952). However, inspection of the publicly available information, including expressed sequence tags s and experimentally identified transcription start sites (TSSs) (http://dbtss.hgc.jp/), suggested the existence of additional mRNAs transcribed from this locus. To identify the hypothetical RNA isoforms encoded by the *EFNA3* locus, we performed 5′-RACE (5′-rapid amplification of cDNA ends) experiments in HeLa and LoVo cell lines (Supplementary Figure 2) and found two TSSs in addition to that of the NM_004952 mRNA (Figure 1b). The existence and location of these additional TSSs was supported by 5′ cap analysis gene expression tags from multiple cell lines produced as part of the ENCODE Transcriptome Project (Supplementary Figure 2). Interestingly, none of these novel RNAs seemed to encode for functional proteins and, accordingly, we termed them noncoding-1 (NC1) and NC2, based on their different TSSs (Figure 1b). Specifically, NC1 isoform contains an ATG codon within its first 10 nucleotides that is in frame with the

open reading frames of NM_004952, suggesting that NC1 could encode a truncated form of Ephrin A3. However, this potential product would have an interrupted structural domain (the ephrin domain) that makes up the bulk of the protein, which would likely undermine its stability. On the other hand, the NC2 sequence does not contain any open reading frames of significant length. In agreement, *in vitro* transcription-coupled translation of *EFNA3* and NC1 cDNAs produced the proteins of expected sizes, whereas NC2 cDNA generated no apparent protein product (Figure 1c and Supplementary Figure 3A). To test the coding potential of NC1 and NC2 in intact cells, we transfected HeLa cells with the respective plasmids along with the canonical *EFNA3* cDNA (*EFNA3*) (Figure 1d and Supplementary Figures 3B and C). Neither NC1 nor NC2 caused the expression of exogenous protein that could be recognized by the monoclonal or polyclonal antibody against *EFNA3*. Thus, NC1 and NC2 can be considered novel lncRNAs. In addition to the novel TSS, a method using support vector machine for poly(A) site prediction[26] identifies two potential 3′ ends for this locus (Supplementary Figure 2; 'Poly(A) Sites' track). In agreement, analysis of paired-end diTag (PET) sequencing data from ENCODE[27] indicates that all combinations of the TSSs and 3′ ends are present in cells (Supplementary Figure 2; 'GIS-PET' track). Thus, both NC1 and NC2 can be expressed as shorter forms with a truncated 3′-untranslated region, which we termed NC1s and NC2s, respectively (Figure 1b).

We next investigated the regulation by hypoxia of the different transcripts encoded by the *EFNA3* locus. First, we used commercially available TaqMan probes to amplify the regions of the *EFNA3* gene specific to the canonical *EFNA3* mRNA (TaqMan1+2; Figure 1e) and a region common to all the RNA isoforms encoded by this locus (TaqMan4+5; Figure 1e). Quantitative PCR (qPCR) results indicate that the absolute expression levels and relative induction in response to hypoxia varied widely between RNA species (Figure 1e). The expression of the canonical coding isoform was low, compared with the combined expression level for all isoforms, suggesting that under normoxic conditions the transcription of the lncRNAs predominates. This result was confirmed by the ENCODE genome-wide transcription analysis (Supplementary Figure 2; 'Transcription' track). Strikingly, the canonical *EFNA3* isoform was barely induced in response to hypoxia, in stark contrast with the robust upregulation of the bulk of *EFNA3* RNAs (Figure 1e). This result suggested that the lncRNAs, but not the canonical mRNA, were regulated by hypoxia. To confirm this possibility, we designed primer pairs for all the exons in the gene to determine the response to hypoxia of every potential RNA isoform. Indeed, hypoxia strongly upregulated the novel lncRNA isoforms, whereas the regulation of the canonical protein-coding mRNA was only marginal (Figure 1f). Importantly, the induction of *EFNA3* transcripts in response to hypoxia was mediated by HIF as it was blocked by small interfering RNA (siRNA) directed against HIF1α (Figure 1g and Supplementary Figure 4). To investigate the regulation of *EFNA3* by HIF *in vivo*, we used conditional VHL-knockout mouse lines.[28] VHL deletion results in constitutive HIF activity and, consistently with the in vitro results, this led to increased *EFNA3* lncRNA expression without significantly altering the level of the coding *EFNA3* mRNA (Figure 1h). Importantly, the induction of *EFNA3* upon VHL loss was partially prevented in animals lacking both VHL and EPAS (HIF2α) alleles (Figure 1h), suggesting that the *in vivo* HIF2α regulates EFNA3 expression, at least in the liver and the lung. Regardless of the specific HIF isoform involved, which could just

reflect their differential tissue expression, it is clear from these set of results that EFNA3 expression is induced, both in vitro and in vivo, in response to hypoxia, in an HIF-dependent manner.

Mounting evidence indicates that lncRNAs are key regulators of gene expression that affect mRNA transcription rate, stability and translation.[29,30] Thus, in an attempt to reconcile the induction of Ephrin-A3 protein with the regulation of coding and noncoding transcripts by hypoxia, we tested whether NC1 and NC2 lncRNAs could affect *EFNA3* mRNA or protein levels. As shown in Figure 2a, the overexpression of the lncRNAs (Supplementary Figure 5A) had no significant effect on *EFNA3* mRNA levels. However, exogenous expression of NC1/2, particularly the short isoforms (NC1s and NC2s), caused *EFNA3* protein accumulation (Figures 2b and c). To confirm these results, we infected MDA-MB-231 cells with lentivirus encoding for the *EFNA3*-derived lncRNAs (Supplementary Figure 5B) and found a dose-dependent effect of viral infection on Ephrin-A3 protein levels (Figure 2d). These results provide an explanation for the induction of *EFNA3* protein under hypoxia in spite of its modest effect on *EFNA3* mRNA level. As for the mechanism by which *EFNA3* lncRNA promote Ephrin-A3 protein accumulation, we disregarded an effect on protein stability because Ephrin-A3 has a long half-life (over 22 h in HeLa cells, data not shown) and instead considered the possibility that they could affect Ephrin-A3 translation. It is known that miR-210, which is induced by hypoxia,[31,32] prevents the translation of several mRNA including *ISCU* and *EFNA3*.[33–36] As miR-210 binds the 3′-untranslated region of the *EFNA3* mRNA,[34] it is feasible that EFNA3 lncRNAs increase *EFNA3* mRNA translation by depleting miR-210 and other microRNAs (miRNAs) that target the *EFNA3* 3′-untranslated region (Supplementary Figure 2A; TargetScan miRNA track). To test this possibility, we interfered with the miRNA processing machinery by knocking down *DGCR8*, an essential component of the microprocessor complex.[37] As shown in Figure 2e, the interference of *DGCR8* in normoxia resulted in Ephrin-A3 protein accumulation without significantly altering *EFNA3* mRNA levels (Figure 2f and Supplementary Figure 5C). Moreover, *DGCR8* silencing does result in a further increase in Ephrin-A3 protein levels under hypoxia (Figure 2e), suggesting that lncRNAs and miR-210 act on the same pathway Thus, we propose a mechanism by which hypoxia induces *EFNA3* lncRNAs that act as endogenous competing RNAs that relieve *EFNA3* mRNA from miRNA inhibition allowing for efficient transcription.

HIF binding to an intragenic regulatory region induces the transcription of *EFNA3* lncRNAs and, indirectly, regulates Ephrin-A3 expression posttranscriptionally

The different TSSs of the *EFNA3* isoforms suggested the existence of alternative promoters. In agreement, histone modifications landscape, location of the open chromatin and transcription factor binding site regions in the *EFNA3* locus (Figure 3a) were consistent with the existence of two promoter regions (Figure 3a), Prm1and Prm2. To further investigate the regulation of the different *EFNA3* transcripts, we analyzed the binding of RNA polymerase II (Pol II) to these putative promoter regions. As controls, we also included the promoter regions of a *bona fide* hypoxia-inducible gene (*P4HA*) and a non-responsive gene (*STT3A*). Chromatin immunoprecipitation-qPCR (ChIP-qPCR) analysis showed that Pol II bound to both regions of the *EFNA3* gene locus under normoxia (Figure 3b). Consistent with the

relatively low *EFNA3* expression in HeLa cells, the binding of Pol II to the EFNA3 promoter regions was lower than its binding to the *P4HA* and *STT3A* promoters. Importantly, Pol II binding to the Prm2 region was strongly induced by hypoxia (Figure 3b), to a level comparable to the HIF-responsive promoter of *P4HA*. In contrast, the Pol II binding to the Prm1 region and to the *STT3A* promoter remained unaffected by hypoxia (Figure 3b).

Next, we investigated direct binding of HIF1α to the *EFNA3* locus by ChIP-qPCR. We designed six primer sets (Figure 3a), H1–H6, to sample most of the RCGTG motifs (Figure 3a; 'RCGTG motifs' track) within *EFNA3* locus and found that the only fragment that showed significant HIF binding under hypoxic conditions was H6 (Figure 3c). Interestingly, H6 region is in close proximity to Prm2, which could explain the differential response of promoter regions 1 and 2 to hypoxia.

Finally, we cloned both *EFNA3* promoter regions and studied their response to hypoxia and to the chemical inhibitor of HIF prolyl hydroxylases, dimethyloxalylglycine (DMOG), which causes acute HIF activation. Although both regions showed similar basal promoter activity (data not shown), Prm2 was strongly induced by hypoxia and DMOG, whereas Prm1 remained unaffected (Figure 3d). Importantly, Prm2 response to hypoxia was critically dependent on one of its RCGTG motifs whose mutation completely abrogated hypoxic induction (Figure 3d).

HIF activation correlates with *EFNA3* expression in human tumors Over 80% of human ccRCC samples are deficient for VHL function and, as a consequence, present constitutive HIF activity even in the presence of oxygen.[14] Thus, ccRCC is highly suitable to study a putative link between HIF and *EFNA3* in human tumors. In agreement, the expression of EGLN3, a well-characterized direct target of HIF, was clearly increased in the three independent ccRCC tumor series (Figure 4a). Similarly, *EFNA3* was significantly increased in ccRCC tumor cells as compared with the normal kidney tissue in the same series, regardless of the microarray platform used to assay tumor samples (Figure 4b). The probes used to determine *EFNA3* expression in these data sets bind to regions common to all transcripts from this locus (see Materials and methods), and thus they detect the cumulative signal by the mRNA and lncRNA transcripts. However, as the expression of lncRNAs was much higher than that of *EFNA3* mRNA in all cell types and tissues tested so far (Figure 1, Supplementary Figure 2 and data not shown), we assume that the microarray signal is largely generated by the lncRNA. We also examined the expression of two other EFNA family members, *EFNA1* and *EFNA4*, whose coding genes flank the *EFNA3* locus in mammalian genomes. Interestingly, *EFNA1*, but not *EFNA4*, is induced by hypoxia (Yamashita *et al.*[24] and data not shown). Concordantly, the expression of *EFNA1*, but not that of *EFNA4*, is clearly increased in ccRCC (Figure 4). These results rule out that the increased *EFNA3* expression observed in these tumors could be caused by a gross structural alteration or transcriptional deregulation of the genomic region containing the *EFNA3* gene and suggest that it is due to increased HIF activity, as it correlates with the changes observed for other hypoxia-regulated genes.

EFNA3 promotes metastatic behavior by enhancing extravasation of tumor cells

As hypoxia is a common condition in solid tumors that correlates with metastatic potential[2] and some ephrin family members have been implicated in the promotion of metastatic behavior,[21] we next studied the metastatic potential of MDA-MB-231 cells engineered to express luciferase and *EFNA3* in an orthotopic xenotransplantation model. At 5 weeks after tumor inoculation, the total photon flux was significantly higher in most animals bearing *EFNA3*-positive tumors, compared with controls (Figures 5a and b). Importantly, the luminiscence signal in *EFNA3* animals was not restricted to the original injection site but diffused throughout the abdominal area, suggesting metastatic spread rather than increased primary tumor growth. In agreement, the volumes of the primary tumors did not differ significantly between groups at the end of the experiment (Figure 5c) and necropsies confirmed that seven out of eight of the animals injected with *EFNA3*-positive cells presented with metastases as opposed to one out of seven in the control group (Figure 5d). Most metastases were located in the peritoneal cavity, attached to the surface of internal organs (Figure 5e). The increased metastatic potential of the expressing cells was confirmed in another mouse metastasis model where the same cells were injected via the tail vein to generate experimental lung metastases (Supplementary Figure 6).

Importantly, the microvascular density, as determined by analysis of CD31 staining, was similar between the *EFNA3*-positive and -negative tumors (Figures 5f and g). Thus, the increased metastatic potential of *EFNA3*-expressing cells was not due to increased vascular density. Ephrins, through their receptors, mediate attraction and repulsion signals between cells.[17] This function could enable tumor cells entry and exit from blood vessels and in this way increase their metastatic potential. To test this possibility, we plated HEK293T cells, transiently transfected with plasmids encoding *EFNA3*, on top of the human umbilical vein endothelial cell (HUVEC) grown as a cell monolayer and measured the ability of HEK-*EFNA3* cells to pass through HUVEC monolayer and attach to the plastic surface below. As shown in Figures 6a and b, the number of GFP-positive cells attached and spread on the plate was significantly higher when *EFNA3* was expressed. These results are consistent with *Ephrin*-A3 transducing a repulsive signal to HUVECs that allowed HEK293T cells to transmigrate through the monolayer. In agreement, recombinant Ephrin-A3-Fc blocked the directional migration of HUVECs induced by the conditioned media from NIH 3T3 cells (Figure 6c).

These data suggest a mechanism for the increased metastatic potential of the tumors cells expressing *EFNA3* whereby they can efficiently intravasate and extravasate through the vascular wall. To investigate this possibility *in vivo*, we injected MDA-MB-231 cells in the tail vein of immunodeficient mice and assessed the appearance of the individual tumoral cells in the lungs in a short-term assay. Although the number of circulating tumor cells 2 h after injection was similar in the control and experimental groups, 7 days later the GFP signal was much higher in the animals injected with *EFNA3*-expressing cells (Figures 6d and e). Collectively, these results suggest that Ephrin-A3 facilitates metastasis, at least in part, by allowing the extravasation of the tumor cells from the vasculature.

As the upregulation of Ephrin-A3 protein by hypoxia is mediated by the induction of *EFNA3* lncRNAs, we next sought to investigate their effect on the metastatic potential of MDA-MB-231 cells. To that end, we generated cell lines overexpressing all the different transcripts from the *EFNA3* locus and tested them in a zebrafish metastasis model.[38,39] In agreement with the mouse models, expression of EFNA3 mRNA significantly increased the metastatic ability of MDA-MB-231 cells, as determined by the number of disseminated cells from the perivitelline cavity to the tail region of fish embryos (Figure 7). This result confirms that Ephrin-A3 induced metastatic properties in very different model systems. Furthermore, this model allows the detection of individual metastatic cells in close association with the blood vessels (Figure 7a, white arrows), which resembles the results obtained in the lung seeding assay (Figures 6d and e). Importantly, overexpression of any of the lncRNAs was sufficient to promote the dissemination of tumor cells to a degree similar, or even higher, to that conferred by *EFNA3* mRNA. In agreement, the migration of HEK293T cells through a monolayer of endothelial cells was enhanced by the expression of *EFNA3* lncRNAs (Supplementary Figure 7). Thus, the expression of either *EFNA3* mRNA or lncRNA is sufficient to promote metastatic behavior.

In view of these results, we next analyzed the correlation between *EFNA3* expression and the risk of metastasis in breast cancer patients. To this end, we made use of the public access data sets of human breast cancer gene expression and associated clinical data from the ROCK website (Online Breast Cancer Knowledgebase; http://www.rock.icr.ac.uk/).[40] We categorized patient samples according to *EFNA3* expression level (high vs low) and analyzed the incidence of metastasis over time in both groups (Figure 8). In agreement with the results of the animal studies, the risk of metastatic disease was significantly higher in patients whose primary tumors expressed higher levels of *EFNA3* (Figure 8).

DISCUSSION

The majority of known HIF targets are regulated by direct induction of coding mRNA. In this study, using Ephrin A3 as an example, we suggest a novel way of hypoxic regulation of gene expression whereby the changes in the coding mRNA are only marginal. In this model, HIF directly regulates the levels of lncRNAs, which, in turn, increase protein levels by acting as competing endogenous RNAs that sequester miRNAs away from *EFNA3* mRNA allowing for its translation. Interestingly, during the preparation of this manuscript, Choudhry *et al*.[41] reported an unexpected role for hypoxia in regulating lncRNA expression. On the other hand, the role of miRNAs in the hypoxic response is well documented.[42] Thus, it is likely that the complex mechanism described herein is not an isolated case but a more general theme in the regulation of gene expression by oxygen.

In spite of our data, further work is needed to fully understand the mechanism by which hypoxia regulates Ephrin-A3 expression. For example, a recent report describes how lncRNA that affects Uchl1 protein levels by enhancing mRNA translation of the coding mRNA.[43] Therefore, we cannot formally rule out that *EFNA3*-encoded lncRNAs directly regulate *EFNA3* mRNA translation rate. Similarly, we have not explored the possibility that *EPAS1* could contribute to the accumulation of Ephrin-A3 during hypoxia by increasing its translation as has been reported for the EGFR.[44] Finally, we cannot completely discard an

effect of hypoxia on *EFNA3* mRNA transcription. Although the effect of hypoxia on *EFNA3* mRNA level was relatively small in HeLa and MDA-MB-231 cells, and not detectable in VHL-deficient mice, we observed higher inductions in other cell lines such as LoVo and MCF7 (data not shown). As we found no evidences of regulation of EFNA3 mRNA by HIF (Figure 3), the induction of *EFNA3* mRNA by hypoxia could be a consequence of the different effects of miRNAs on gene expression, ranging from inhibition of translation to decrease mRNA stability. For example, as the relative proportion of the miRNAs binding to *EFNA3* mRNA varies in different cell lines or conditions, their net effect on *EFNA3* mRNA could change from preventing translation to affecting mRNA half-life. Alternatively, lncRNAs could also mediate the transcriptional induction of EFNA mRNA in a cell-specific manner.[29,30] At any rate, our results highlight that EFNA3 response to hypoxia is tightly controlled and lncRNA induction has a key role on its regulation.

Regarding the mechanism responsible for the selective transcription of specific *EFNA3* isoforms, we found that it is mediated by discriminatory recruitment of HIF and RNA Pol II to the Prm2 promoter region. Interestingly, the presence of CTCF binding sites flanking *EFNA3* Prm2 region (Supplementary Figure 2) offers a plausible explanation for the preferential transcriptional activation of the lncRNA by HIF and the lack of the regulation of the canonical coding isoform. Other studies also demonstrate the role of insulators in determination of HIF specificity for promoters located in close proximity.[45] Also regarding the molecular mechanism, we found that *in vitro EFNA3* induction was dependent on HIF-1α and not affected by HIF-2α knockdown, whereas in animal models, EPAS1 was required for EFNA3A induction upon VHL loss. Thus, HIF isoforms responsible for EFNA3 may be context-dependent and could be dictated by the availability of a specific HIF isoform, or another, HIF cell-type-specific transcription factor(s), that favor interaction with a specific HIF isoform. Nonetheless, this has been observed for other hypoxia-regulated genes. For instance, the hypoxic regulation of another ephrin, Ephrin-A1, also requires HIF1α[22] in cell cultures, but not *in vivo*, where it is dependent on HIF-2α.[24]

An important question arising from our results relates to the role of Ephrin-A3 in the physiologic response to hypoxia. The induction of angiogenesis is one of the classical responses to hypoxia and other ephrins has key roles in angio- and vasculogenesis. However, we did not find a significant effect of Ephrin-A3 expression on tumor vascular density as determined by CD31 staining. Although we cannot rule out effects on other vascular parameters like maturation or normalization of tumor vasculature, our results demonstrate a direct role of Ephrin-A3 on tumor cell intra-/extravasation that could underlie the prometastatic action of this ephrin. Earlier studies showed that Ephrin-A3 overexpression prevents the *in vitro* formation of capillary-like structures by HUVECs.[34,46] We similarly found that recombinant Ephrin-A3-Fc prevents the migration of HUVECs *in vitro*; however, these *in vitro* effects did not manifest in the *in vivo* models.

Regardless of their physiologic role, ephrins are frequently co-opted by the transformed cells whereby they contribute to the changes in cell–cell and cell–matrix attachment and survival during invasion, angiogenesis and metastasis.[17,20] In agreement with this, we found that the expression of Ephrin-A3 in MDA-MB-231 breast cancer cells increased their metastatic potential. The significant correlation that we found between high *EFNA3* levels and

metastasis in clinical samples strongly supports this conclusion. Also in agreement with our findings, a recent study demonstrated the differential expression of Eprin-A3 between the highly metastatic and poorly metastatic colon cancer cells.[47] Although we have not formally demonstrated it, it is tempting to speculate that the correlation of hypoxia with metastasis risk observed in human tumors is, at least in part, explained by the induction of Ephrin-A3 downstream of HIF activation owing to the tumor hypoxia or oncogenic alterations. As for the mechanism, our results suggest that Ephrin-A3 promotes metastasis by repelling vascular endothelium and therefore creating points of intra- and extravasation for the tumor cells. Similar events are caused by angiopoietin-like 4 (*ANGPTL4*), another hypoxia-inducible gene, to promote metastasis.[48] Importantly, we found that the expression of the lncRNAs is sufficient to promote metastasis, highlighting the relevance of this class of transcripts in the control of biologic processes and human disease.

In summary, we demonstrate a novel mechanism of hypoxic regulation, where *EFNA3* expression is driven by previously non-annotated intragenic lncRNAs whose transcription is controlled by HIF. We propose that in hypoxic regions of solid tumors or in tumors harboring genetic alterations leading to constitutively active HIF, this novel mechanism leads to Ephrin-A3 accumulation and the promotion of metastasis.

MATERIALS AND METHODS

Cell culture

Cells were grown in standard culture conditions. For hypoxia treatments, cells were placed in a 1% O_2, 5% CO_2 and 94% N_2 gas mixture in a Whitley hypoxystation (don Whitley Scientific, Bradford, UK). DMOG (Frontier Scientific, Oakland, CA, USA) was added, where indicated, at a 500 μM final concentration. MDA-MB231-EphrinA3-Luc and MDA-MB231-Luc cells were generated by infection with pLOC-EFNA3 or pLOC lentivirus, respectively, and then reinfected with Lenti-Fire Luciferase Luc2 (CellCyto, Beijing, China) lentivirus.

ChIP

ChIP was performed as described previously[49] with minor modifications. Briefly, EZ Chromatin Immunoprecipitation Kit (Millipore, Billerica, MA, USA) was used following the manufacturer's instructions. HeLa cells were grown to 85% confluence on 10 cm plates before they were exposed to hypoxia or left in normoxic conditions. Chromatin was immunoprecipitated with antibodies against RNA Pol II (Abcam, Cambridge, UK; 5408) or Hif1a (Abcam; ab2185). Mouse IgG (Sigma, St Louis, MO, USA; M8695) or whole rabbit serum were used as negative controls. DNA was purified by phenol–chloroform extraction and ethanol precipitation and bound regions were identified by qPCR with indicated primer pairs (Supplementary Tables I and II).

Repulsion assay

HUVEC cells were stained with 10 μM per 10^6 cells of a membrane labeling reagent PKH26 (Sigma), seeded into a 24-multiwell plate (1×10^6 cells per well) and allowed spread to form a cell monolayer overnight. Then, HEK-293T cells, expressing GFP alone or in

combination with Eprhrin-A3, were plated on top of the HUVECs (3000 cells per well) and mixed cell culture followed over time.

Orthotopic tumor implantation, extravasation assays and zebrafish metastasis model

Tumor studies were performed on 5- to 7-week-old female nude mice (Harlan, Indianapolis, IN, USA) according to the protocols in accordance with the NIH Guide for the Care and Use of Laboratory Animals. MDA-MB-231-Luc and MDA-MB-231-EphrinA3-Luc cells were harvested by trypsinization, resuspended in phosphate-buffered saline and injected into the mammary fat pad (10^6 per site, one site per mouse) of immunodeficient mice in a 1:1 mix with Matrigel (BD Biosciences, San Jose, CA, USA). The animals were subjected to weekly bioluminescence imaging in an IVIS Spectrum System (Caliper; Xenogen, Hopkinton, MA, USA) to monitor tumor progression and metastasis. The mice were given intraperitoneal injections of D-luciferin (15 mg/ml in phosphate-buffered saline), 5 min before imaging. Tumors, lungs, bones and livers were harvested after 9 weeks and processed for tissue analysis. Primary tumor volumes were calculated as length × width^2 × 0.52. For the extravasation assays, cells were injected into the tail vein. Extravasation of cells was monitored by confocal images of whole fresh lungs. The metastatic ability of tumor cell lines in the zebrafish metastasis model was assayed as described by Rouhi *et al*.[38,39]

Gene expression profile analysis

Gene expression data and relevant sample information were downloaded from the Gene Expression Omnibus (http://www.ncbi.nlm.nih.gov/geo/) and ROCK (http://www.rock.icr.ac.uk/) databases (free public access) and analyzed using custom scripts written in R language.

Statistical analysis

Statistical analysis and graphic representations were performed in R, a language and environment for statistical computation and graphics.[50]

Supplementary Material

Refer to Web version on PubMed Central for supplementary material.

Acknowledgments

We thank Amparo Acker-Palmer for expert advice on ephrin detection and Ignacio Palmero DGCR8 reagents. This work was supported by Ministerio de Ciencia e Innovación (Spanish Ministry of Science and Innovation, MICINN) (grant numbers SAF2008-03147 and SAF2011_24225 to LdelP and SAF-2010-19256 to BJ); by Comunidad Autónoma de Madrid (grant numbers S2010/BMD-2542 to LdelP), by the 7th Research Framework Programme of the European Union (grant number METOXIA project ref. HEALTH-F2-2009-222741 to LdelP); by CSIC (JAE DOC 2010/FSE2007-2013 to OR) and by Fondo de Investigación Sanitaria/Instituto de Salud Carlos III (grants PI08/90856 and PS09/00227 to LS).

REFERENCES

1. Bertout JA, Patel SA, Simon MC. The impact of O_2 availability on human cancer. Nat Rev Cancer. 2008; 8:967–975. [PubMed: 18987634]
2. Vaupel P, Mayer A. Hypoxia in cancer: significance and impact on clinical outcome. Cancer Metast Rev. 2007; 26:225–239.

3. Wang GL, Jiang BH, Rue Ea, Semenza GL. Hypoxia-inducible factor 1 is a basic-helix-loop-helix-PAS heterodimer regulated by cellular O_2 tension. Proc Natl Acad Sci USA. 1995; 92:5510–5514. [PubMed: 7539918]
4. Kaelin WG, Ratcliffe PJ. Oxygen sensing by metazoans: the central role of the HIF hydroxylase pathway. Mol Cell. 2008; 30:393–402. [PubMed: 18498744]
5. Epstein AC, Gleadle JM, McNeill LA, Hewitson KS, O'Rourke J, Mole DR, et al. *C. elegans* EGL-9 and mammalian homologs define a family of dioxygenases that regulate HIF by prolyl hydroxylation. Cell. 2001; 107:43–54. [PubMed: 11595184]
6. Salceda S, Caro J. Hypoxia-inducible factor 1alpha (HIF-1alpha) protein is rapidly degraded by the ubiquitin–proteasome system under normoxic conditions Its stabilization by hypoxia depends on redox-induced changes. J Biol Chem. 1997; 272:22642–22647. [PubMed: 9278421]
7. Hewitson KS, McNeill La, Riordan MV, Tian Y-M, Bullock AN, Welford RW, et al. Hypoxia-inducible factor (HIF) asparagine hydroxylase is identical to factor inhibiting HIF (FIH) and is related to the cupin structural family. J Biol Chem. 2002; 277:26351–26355. [PubMed: 12042299]
8. Jiang BH, Zheng JZ, Leung SW, Roe R, Semenza GL. Transactivation inhibitory domains of hypoxia-inducible factor 1alpha Modulation of transcriptional activity by oxygen tension. J Biol Chem. 1997; 272:19253–19260. [PubMed: 9235919]
9. Lando D, Peet DJ, Whelan Da, Gorman JJ, Whitelaw ML. Asparagine hydroxylation of the HIF transactivation domain a hypoxic switch. Science. 2002; 295:858–861. [PubMed: 11823643]
10. Semenza GL. Targeting HIF-1 for cancer therapy. Nat Rev Cancer. 2003; 3:721–732. [PubMed: 13130303]
11. Ivan M, Kondo K, Yang H, Kim W, Valiando J, Ohh M, et al. HIFalpha targeted for VHL-mediated destruction by proline hydroxylation: implications for O_2 sensing. Science. 2001; 292:464–468. [PubMed: 11292862]
12. Jaakkola P, Mole DR, Tian YM, Wilson MI, Gielbert J, Gaskell SJ, et al. Targeting of HIF-alpha to the von Hippel-Lindau ubiquitylation complex by O_2-regulated prolyl hydroxylation. Science. 2001; 292:468–472. [PubMed: 11292861]
13. Maxwell PH, Wiesener MS, Chang GW, Clifford SC, Vaux EC, Cockman ME, et al. The tumour suppressor protein VHL targets hypoxia-inducible factors for oxygen-dependent proteolysis. Nature. 1999; 399:271–275. [PubMed: 10353251]
14. Kaelin WG. Von Hippel-Lindau disease. Annu Rev Pathol. 2007; 2:145–173. [PubMed: 18039096]
15. Semenza GL. Hypoxia-inducible factors: mediators of cancer progression and targets for cancer therapy. Trends Pharmacol Sci. 2012; 33:207–214. [PubMed: 22398146]
16. Lu X, Kang Y. Hypoxia and hypoxia-inducible factors: master regulators of metastasis. Clin Cancer Res. 2010; 16:5928–5935. [PubMed: 20962028]
17. Nievergall E, Lackmann M, Janes PW. Eph-dependent cell-cell adhesion and segregation in development and cancer. Cell Mol Life Sci. 2012; 69:1813–1842. [PubMed: 22204021]
18. Pasquale EB. Eph receptors and ephrins in cancer: bidirectional signalling and beyond. Nat Rev Cancer. 2010; 10:165–180. [PubMed: 20179713]
19. Pasquale EB. Eph-ephrin bidirectional signaling in physiology and disease. Cell. 2008; 133:38–52. [PubMed: 18394988]
20. Chen J. Regulation of tumor initiation and metastatic progression by Eph receptor tyrosine kinases. Adv Cancer Res. 2012; 114:1–20. [PubMed: 22588054]
21. Surawska H, Ma PC, Salgia R. The role of ephrins and Eph receptors in cancer. Cytokine Growth Factor Rev. 2004; 15:419–433. [PubMed: 15561600]
22. Vihanto MM, Plock J, Erni D, Frey BM, Frey FJ, Huynh-Do U. Hypoxia up-regulates expression of Eph receptors and ephrins in mouse skin. FASEB J. 2005; 19:1689–1691. [PubMed: 16081502]
23. Ogawa K, Pasqualini R, Lindberg RA, Kain R, Freeman AL, Pasquale EB. The ephrin-A1 ligand and its receptor, EphA2, are expressed during tumor neo-vascularization. Oncogene. 2000; 19:6043–6052. [PubMed: 11146556]
24. Yamashita T, Ohneda K, Nagano M, Miyoshi C, Kaneko N, Miwa Y, et al. Hypoxia-inducible transcription factor-2alpha in endothelial cells regulates tumor neovascularization through activation of ephrin A1. J Biol Chem. 2008; 283:18926–18936. [PubMed: 18434321]

25. Ortiz-Barahona A, Villar D, Pescador N, Amigo J, del Peso L. Genome-wide identification of hypoxia-inducible factor binding sites and target genes by a probabilistic model integrating transcription-profiling data and in silico binding site prediction. Nucleic Acids Res. 2010; 38:2332–2345. [PubMed: 20061373]
26. Cheng Y, Miura RM, Tian B. Prediction of mRNA polyadenylation sites by support vector machine. Bioinformatics. 2006; 22:2320–2325. [PubMed: 16870936]
27. Ng P, Wei C, Sung W, Chiu KP, Lipovich L, Ang CC, et al. Gene identification signature (GIS) analysis for transcriptome characterization and genome annotation. Nat Methods. 2005; 2:105–111. [PubMed: 15782207]
28. Miró-Murillo M, Elorza A, Soro-Arnáiz I, Albacete-Albacete L, Ordoñez A, Balsa E, et al. Acute Vhl gene inactivation induces cardiac HIF-dependent erythropoietin gene expression. PLoS One. 2011; 6:e22589. [PubMed: 21811636]
29. Nie L, Wu H, Hsu J-M, Chang S, Labaff AM, Li C, et al. Long non-coding RNAs: versatile master regulators of gene expression and crucial players in cancer. Am J Transl Res. 2012; 4:127–150. [PubMed: 22611467]
30. Yoon J-H, Abdelmohsen K, Gorospe M. Posttranscriptional gene regulation by long noncoding RNA. J Mol Biol. 2013; 425:3723–3730. [PubMed: 23178169]
31. Huang X, Ding L, Bennewith KL, Tong RT, Welford SM, Ang KK, et al. Hypoxia-inducible mir-210 regulates normoxic gene expression involved in tumor initiation. Mol Cell. 2009; 35:856–867. [PubMed: 19782034]
32. Kulshreshtha R, Ferracin M, Wojcik SE, Garzon R, Alder H, Agosto-Perez FJ, et al. A microRNA signature of hypoxia. Mol Cell Biol. 2007; 27:1859–1867. [PubMed: 17194750]
33. Chan SY, Zhang Y-Y, Hemann C, Mahoney CE, Zweier JL, Loscalzo J. MicroRNA-210 controls mitochondrial metabolism during hypoxia by repressing the iron-sulfur cluster assembly proteins ISCU1/2. Cell Metab. 2009; 10:273–284. [PubMed: 19808020]
34. Fasanaro P, D'Alessandra Y, Di Stefano V, Melchionna R, Romani S, Pompilio G, et al. MicroRNA-210 modulates endothelial cell response to hypoxia and inhibits the receptor tyrosine kinase ligand Ephrin-A3. J Biol Chem. 2008; 283:15878–15883. [PubMed: 18417479]
35. Favaro E, Ramachandran A, McCormick R, Gee H, Blancher C, Crosby M, et al. MicroRNA-210 regulates mitochondrial free radical response to hypoxia and krebs cycle in cancer cells by targeting iron sulfur cluster protein ISCU. PLoS One. 2010; 5:e10345. [PubMed: 20436681]
36. Huang X, Le Q-T, Giaccia AJ. MiR-210—micromanager of the hypoxia pathway. Trends Mol Med. 2010; 16:230–237. [PubMed: 20434954]
37. Fukaya T, Tomari Y. MicroRNAs mediate gene silencing via multiple different pathways in *Drosophila* . Mol Cell. 2012; 48:825–836. [PubMed: 23123195]
38. Rouhi P, Jensen LD, Cao Z, Hosaka K, Länne T, Wahlberg E, et al. Hypoxia-induced metastasis model in embryonic zebrafish. Nat Protoc. 2010; 5:1911–1918. [PubMed: 21127485]
39. Rouhi P, Lee SLC, Cao Z, Hedlund E-M, Jensen LD, Cao Y. Pathological angiogenesis facilitates tumor cell dissemination and metastasis. Cell Cycle. 2010; 9:913–917. [PubMed: 20160500]
40. Sims D, Bursteinas B, Gao Q, Jain E, MacKay A, Mitsopoulos C, et al. ROCK: a breast cancer functional genomics resource. Breast Cancer Res Treat. 2010; 124:567–572. [PubMed: 20563840]
41. Choudhry H, Schödel J, Oikonomopoulos S, Camps C, Grampp S, Harris AL, et al. Extensive regulation of the non-coding transcriptome by hypoxia: role of HIF in releasing paused RNApol2. EMBO Rep. 2014; 15:70–76. [PubMed: 24363272]
42. Nallamshetty S, Chan SY, Loscalzo J. Hypoxia: a master regulator of microRNA biogenesis and activity. Free Radic Biol Med. 2013; 64:20–30. [PubMed: 23712003]
43. Carrieri C, Cimatti L, Biagioli M, Beugnet A, Zucchelli S, Fedele S, et al. Long non-coding antisense RNA controls Uchl1 translation through an embedded SINEB2 repeat. Nature. 2012; 491:454–457. [PubMed: 23064229]
44. Uniacke J, Holterman CE, Lachance G, Franovic A, Jacob MD, Fabian MR, et al. An oxygen-regulated switch in the protein synthesis machinery. Nature. 2012; 486:126–129. [PubMed: 22678294]

45. Tiana M, Villar D, Pérez-Guijarro E, Gómez-Maldonado L, Moltó E, Fernández-Miñán A, et al. A role for insulator elements in the regulation of gene expression response to hypoxia. Nucleic Acids Res. 2011; 40:1916–1927. [PubMed: 22067454]

46. Xiao F, Qiu H, Zhou L, Shen X, Yang L, Ding K. WSS25 inhibits Dicer, downregulating microRNA-210, which targets Ephrin-A3, to suppress human microvascular endothelial cell (HMEC-1) tube formation. Glycobiology. 2013; 23:524–535. [PubMed: 23322395]

47. Barderas R, Mendes M, Torres S, Bartolomé RA, López-Lucendo M, Villar-Vázquez R, et al. In-depth characterization of the secretome of colorectal cancer metastatic cells identifies key proteins in cell adhesion, migration, and invasion. Mol Cell Proteomics. 2013; 12:1602–1620. [PubMed: 23443137]

48. Zhang H, Wong CCL, Wei H, Gilkes DM, Korangath P, Chaturvedi P, et al. HIF-1-dependent expression of angiopoietin-like 4 and L1CAM mediates vascular metastasis of hypoxic breast cancer cells to the lungs. Oncogene. 2012; 31:1757–1770. [PubMed: 21860410]

49. Villar D, Ortiz-Barahona A, Gómez-Maldonado L, Pescador N, Sánchez-Cabo F, Hackl H, et al. Cooperativity of stress-responsive transcription factors in core hypoxia-inducible factor binding regions. PLoS One. 2012; 7:e45708. [PubMed: 23029193]

50. Team, RC. R Core Team. R. A Language and Environment for Statistical Computing. Vienna, Austria: 2010.

51. Loi S, Haibe-Kains B, Desmedt C, Wirapati P, Lallemand F, Tutt AM, et al. Predicting prognosis using molecular profiling in estrogen receptor-positive breast cancer treated with tamoxifen. BMC Genom. 2008; 9:239.

52. Pawitan Y, Bjöhle J, Amler L, Borg A-L, Egyhazi S, Hall P, et al. Gene expression profiling spares early breast cancer patients from adjuvant therapy: derived and validated in two population-based cohorts. Breast Cancer Res. 2005; 7:R953–R964. [PubMed: 16280042]

53. Van de Vijver MJ, He YD, van't Veer LJ, Dai H, Hart AAM, Voskuil DW, et al. A gene-expression signature as a predictor of survival in breast cancer. N Engl J Med. 2002; 347:1999–2009. [PubMed: 12490681]

54. Pescador N, Cuevas Y, Naranjo S, Alcaide M, Villar D, Landzuri MO, et al. Identification of a functional hypoxia-responsive element that regulates the expression of the egl nine homologue 3 (egln3/phd3) gene. Biochem J. 2005; 390:189–197. [PubMed: 15823097]

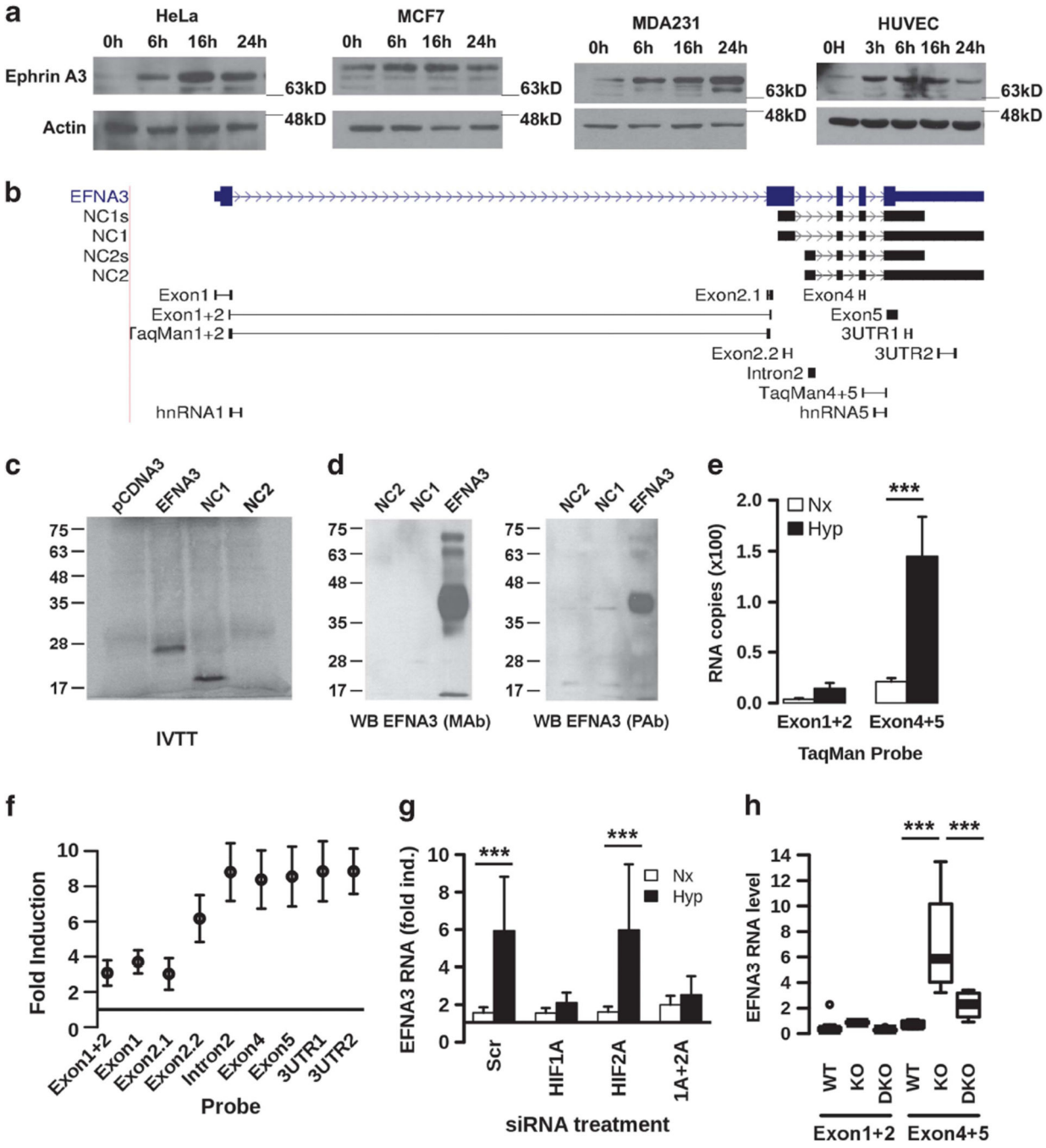

Figure 1.

Hypoxia regulates *EFNA3* expression. (**a**) Ephrin-A3 protein level was determined in HeLa, HUVEC, MCF-7 and MDA-MB231 cells were exposed to normoxia (21% oxygen) or hypoxia (1% oxygen) for the indicated periods of time. (**b**) Diagram of the *EFNA3* locus showing the canonical, NM_004952 RefSeq, gene (upper track, *EFNA3*) and the novel isoforms (second track from the top, NC1–NC2s). The bottom tracks show the position of the qPCR oligonucleotides used in Figures 1d–g (black boxes) and target regions (thin lines). The figure was generated by the UCSC genome browser upon loading the indicated

custom tracks. (**c**) cDNAs corresponding to *EFNA3*, NC1 or NC2 isoforms were transcribed and translated *in vitro* in the presence of ^{35}S-methionine and proteins resolved in a 12% sodium dodecyl sulfate–polyacrylamide gel electrophoresis. Image shows the autoradiogram of a representative experiment. (**d**) HeLa cells were transfected with plasmids encoding for the indicated *EFNA3* isforms and cell lysates probed with monoclonal (mAb) or polyclonal (pAb) antibodies against the C-terminal region of human Ephrin-A3. (**e**) HeLa cells were exposed to 1% oxygen (Hyp) or left at normoxic conditions (Nx) for 12 h and *EFNA3* RNA levels were determined using the indicated TaqMan probes (see panel b). The graph shows the ratio of *EFNA3* to ACTB (β-actin) copy number. Bars represent the mean of three independent biologic replicates and the error bars the s.d. The differences between groups were statistically significant (analysis of variance (ANOVA) $F_{3,8} = 34.21$, $P < 0.001$) and the asterisks indicate means pairs that were the statistically significant (adjusted $P < 0.001$) in *a posteriori* Tukey's test. (**f**) Cells were treated as in (**e**) and *EFNA3* RNA levels were determined using the indicated primer pairs (see panel b). The graph shows the ratio of hypoxic *EFNA3* RNA to the expression in normoxia. Symbols represent the mean of three independent biologic replicates and the error bars the s.d. (**g**) HeLa cells were treated with the indicated siRNAs and then grown at normoxic (21% oxygen, Nx) or hypoxic (1% oxygen, Hyp) conditions for 12 h. The graph represent the normalized levels of *EFNA3* RNA as fold over control conditions (normoxic cells treated with scramble siRNA). Bars represent average values in four independent biologic replicates and error bars the s.d. The differences between groups were statistically significant (ANOVA $F_{7,48} = 23.52$, $P < 0.001$) and the asterisks indicate means pairs that were statistically significant (***adjusted $P < 0.001$) in *a posteriori* Tukey's test. (**h**) Vhlfl/fl-UBC-Cre-ERT2 (n = 5), Vhlfl/flHIF2ocfl/ fl-UBC-Cre-ERT2 ($n = 3$) and control ($n = 11$) mice were placed on a tamoxifen diet for 10 days followed by 10 additional days on a normal diet. The box-and-whisker plot represents the distribution of the normalized *EFNA3* RNA expression in the liver of animals with the indicated genotypes. The box contains the values comprised between the second and third quartiles, and the horizontal black line the median. The 'whiskers' extend to 1.5 times the interquartile range. The differences between groups were statistically significant (ANOVA $F_{2,18} = 20.49$, $P < 0.001$) and the asterisks indicate means pairs that were statistically significant (adjusted $P < 0.001$) in *a posteriori* Tukey's test.

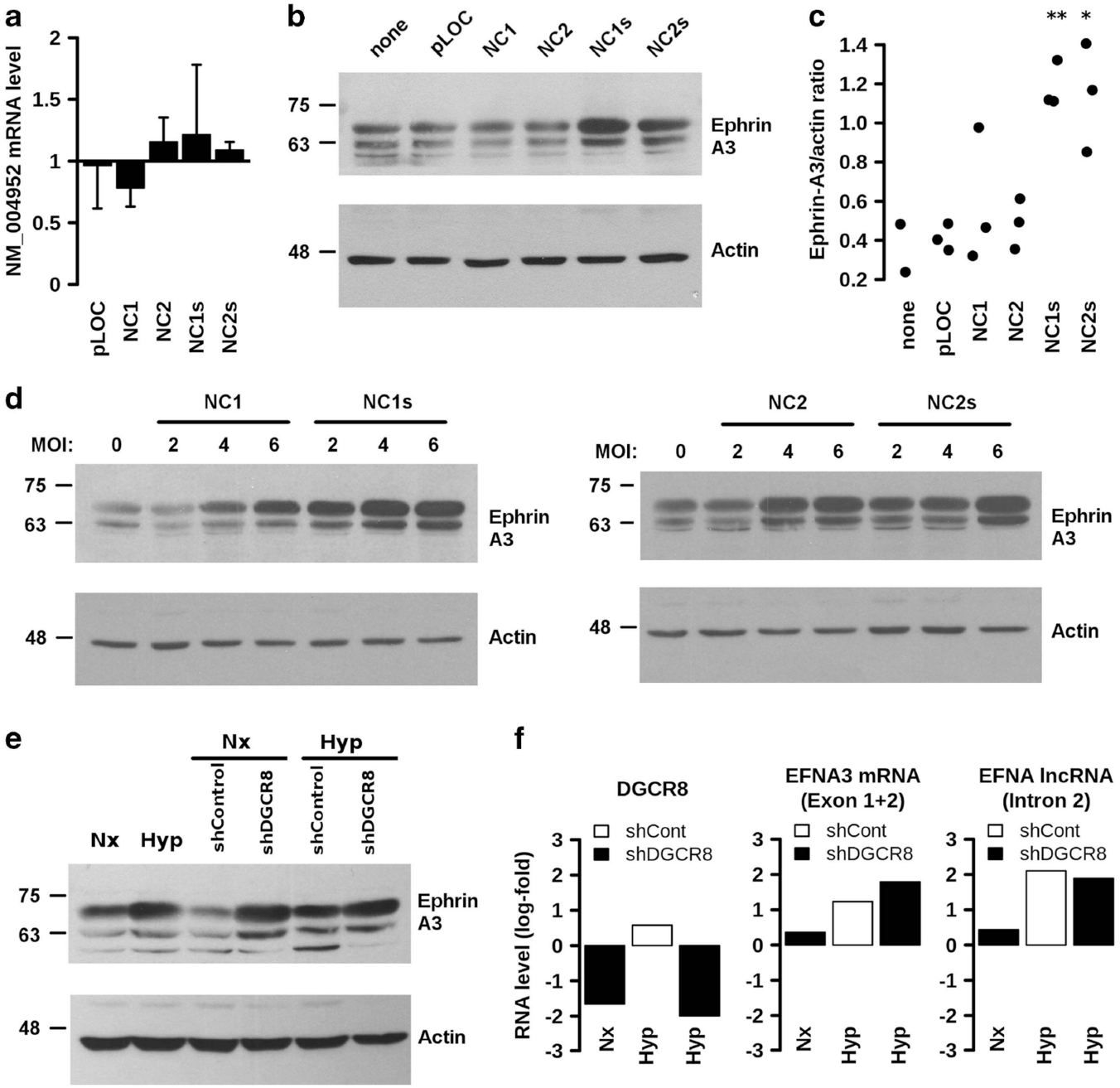

Figure 2.

LncRNA expression results in increased EFNA3 protein levels. HeLa cells were transfected with constructs encoding for the indicated lncRNAs or empty plasmid (pLOC) and the level of the canonical *EFNA3* mRNA (**a**) and protein (**b** and **c**) were determined by qPCR and immunoblot, respectively. The graph in (**a**) represents the level of the NM_004952 mRNA, determined with primers exon 1+2 (Figure 3a), as a fold over the level found in untreated cells. Bars represent the mean of five independent biologic replicates and the error bars the s.d. The differences between groups were not statistically significant (analysis of variance (ANOVA) $F_{4,20} = 1.452$, $P = 0.254$). The graph in (**c**) represents the level of Ephrin-A3 as

the ratio of the Ephrin-A3 band intensity corrected by the actin band intensity in three independent experiments. The differences between groups was statistically significant (ANOVA $F_{5,11} = 8.635$, $P < 0.01$) and the asterisks indicate sample means that were was significantly different from controls (pLOC samples) in a posteriori Tukey's test (*adjusted $P < 0.05$; **adjusted $P < 0.01$). The image in (**b**) is representative of at least three independent experiments. (**d**) MDA-MB-231 cells were infected with lentivus encoding for the indicated constructs at different multiplicity of infection (MOI) and the level of Eprhin-A3 protein was determined by immunoblot. A representative experiment of at least three independent biologic replicas is shown. (**e**) MDA-MB-231 cells were infected with lentiviruses encoding for short hairpin RNA (shRNA) against *DGCR8* (shDGCR8) or control shRNA (shControl) and the level of Eprhin-A3 protein was determined by immunoblot. A representative experiment of two independent biologic replicas is shown. (**f**) The level of *DGCR8* mRNA (DGCR8), *EFNA3* mRNA (EFNA3, exon 1+2) or NC2/NC2 lncRNA (EFNA3, intron 2) in the experiment shown in (**d**) were determined by qPCR.

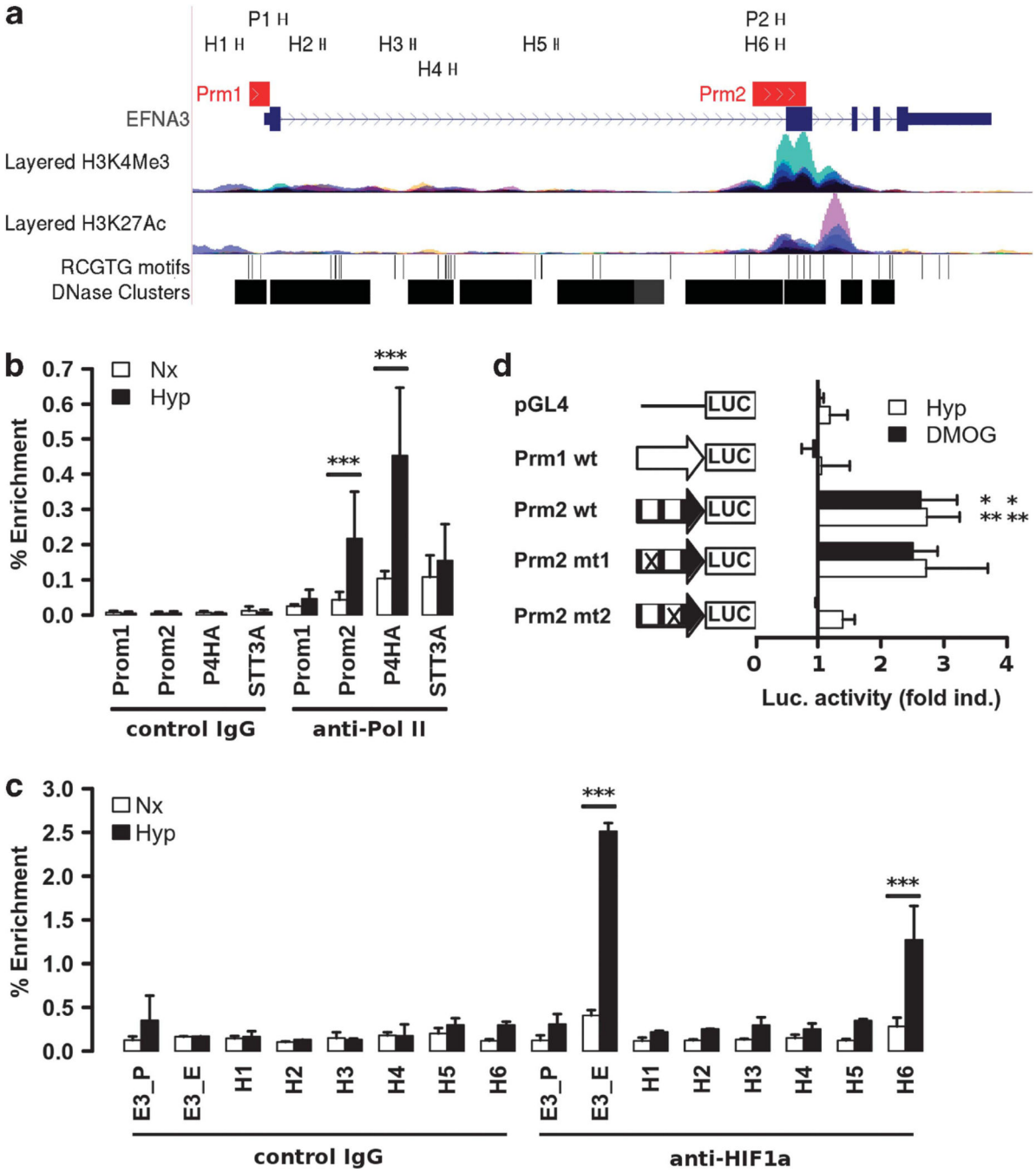

Figure 3.

LncRNAs encoded by the *EFNA* locus are transcribed from an alternative hypoxia-responsive promoter. (**a**) Diagram depicting the *EFNA3* locus and showing the NM_004952 RefSeq gene (‘*EFNA3*’ track) along with accessible chromatin regions (‘DNase clusters track’), histone marks associated with promoters (‘Layered H3K4Me3’ track) and active regulatory elements (‘H3K27Ac Track’). The colors in the histone tracks correspond to the signal obtained in different cell lines (see UCSC genome browser for details). The figure was generated by the UCSC genome browser upon loading custom tracks to indicate the

location of primer and amplicons used in the RNA Pol II (P1 and P2) and Hif1a (H1–H6) ChIP-qPCR experiments as well as the regions cloned to assay their promoter activity ('promoters' track). (**b** and **c**) HeLa cells were exposed to 21 or 1% oxygen for 8 h and RNA Pol II (**b**) or Hif1a (**c**) binding to the indicated regions of the *EFNA3* locus was determined by ChIP-qPCR. Binding to the *P4HA* and *STT3S* promoters were used in the RNA Pol II ChIP experiment as positive and negative controls, respectively. In the case of Hif1a ChIP, the *EGLN3* enhancer region (E3_E) and *EGLN3* promoter region (E3_P) were used as positive and negative controls respectively (Pescador *et* al.[54]). The graphs show the amount of precipitated material as a percentage of the input (%Enrichment). Bars represent the mean of three (**b**) or just one (**c**) independent biologic replicates and the error bars the s.d. The differences between groups were statistically significant (analysis of variance (ANOVA) $F_{15,69}$= 15.6, $P < 0.001$; ANOVA $F_{31,32} = 39.99$, $P < 0.001$) and the asterisks indicate mean pairs that were statistically significant (adjusted $P < 0.001$) in *a posteriori* Tukey's test. (**d**) The effect of hypoxia (white bars) and DMOG (black bars) on the transcriptional activity of the promoter regions 1 and 2 was assessed by reporter assays upon transfection of the indicated constructs into HeLa cells. White boxes within the promoter 2 (Prom2) diagram represent RCGTG motifs and crossed boxes represent deleted RCGTG motifs. The graph shows the normalized luciferase activity in hypoxic (Hyp) or DMOG-treated (DMOG) samples expressed as fold over the activity obtained in normoxic conditions. Bars represent the mean of three (**b**) independent biologic replicates and the error bars the s.d. The differences between groups were statistically significant (ANOVA $F_{4,10} = 21.9$, $P < 0.001$) and the asterisks indicate means pairs that were the statistically significant (*adjusted $P < 0.05$; **adjusted $P < 0.01$) in *a posteriori* Tukey's test.

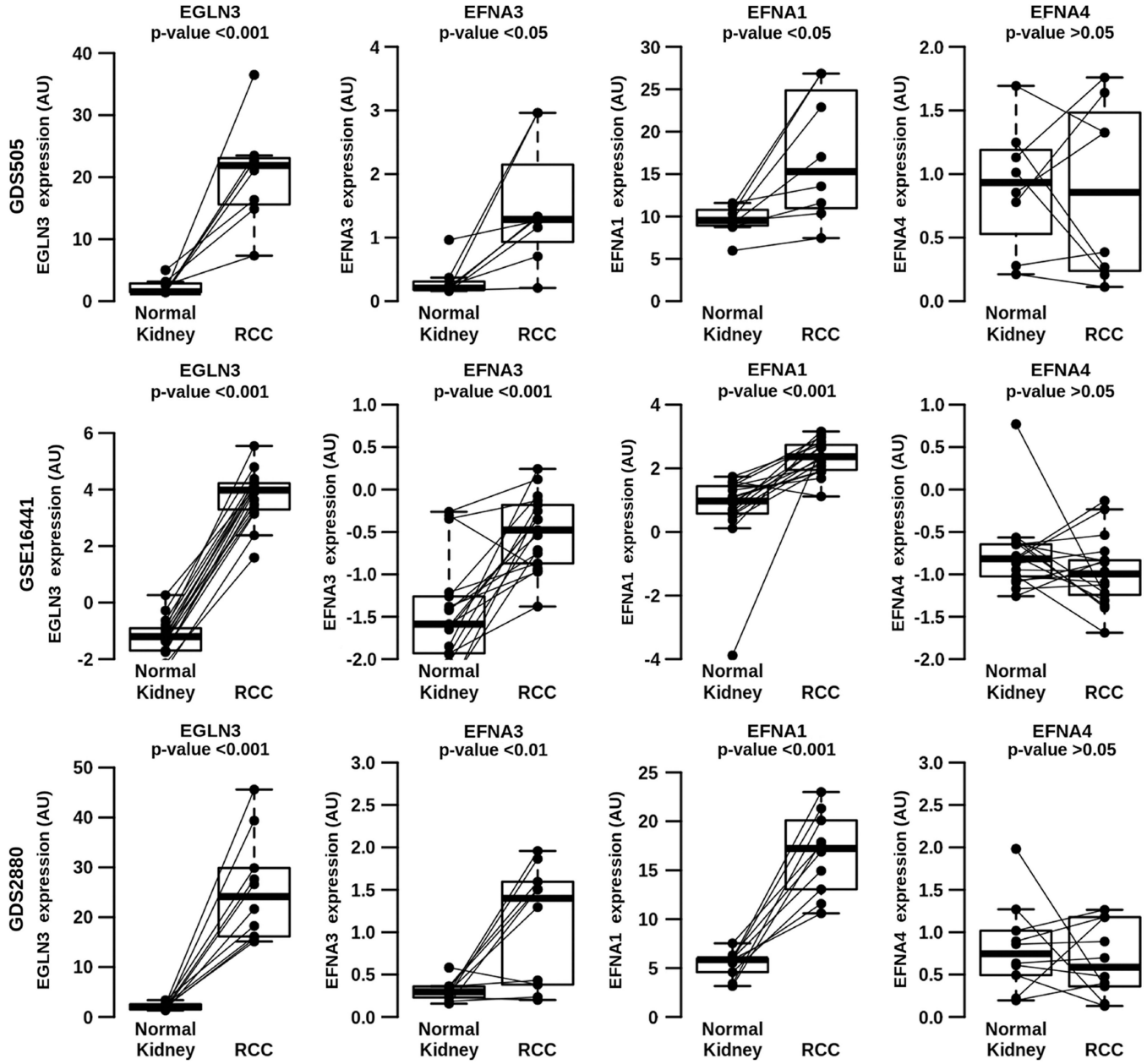

Figure 4.

EFNA3 expression is induced in human RCC. The expression of *EGLN3*, *EFNA3*, *EFNA1* and *EFNA4* (columns) was determined in publicly available gene expression profiles of ccRCC samples from three independent studies (ID shown on the left margin of each row). Graphs represent the expression of the indicated genes in arbitrary units (normalized microarray intensity values). The individual samples are shown and pairs of tumoral and normal kidney tissue are joined by segments. Graphs in each row represent the data from an independent study. The statistical significance of mean differences is indicated on top of each graph (paired Student's *t*-test).

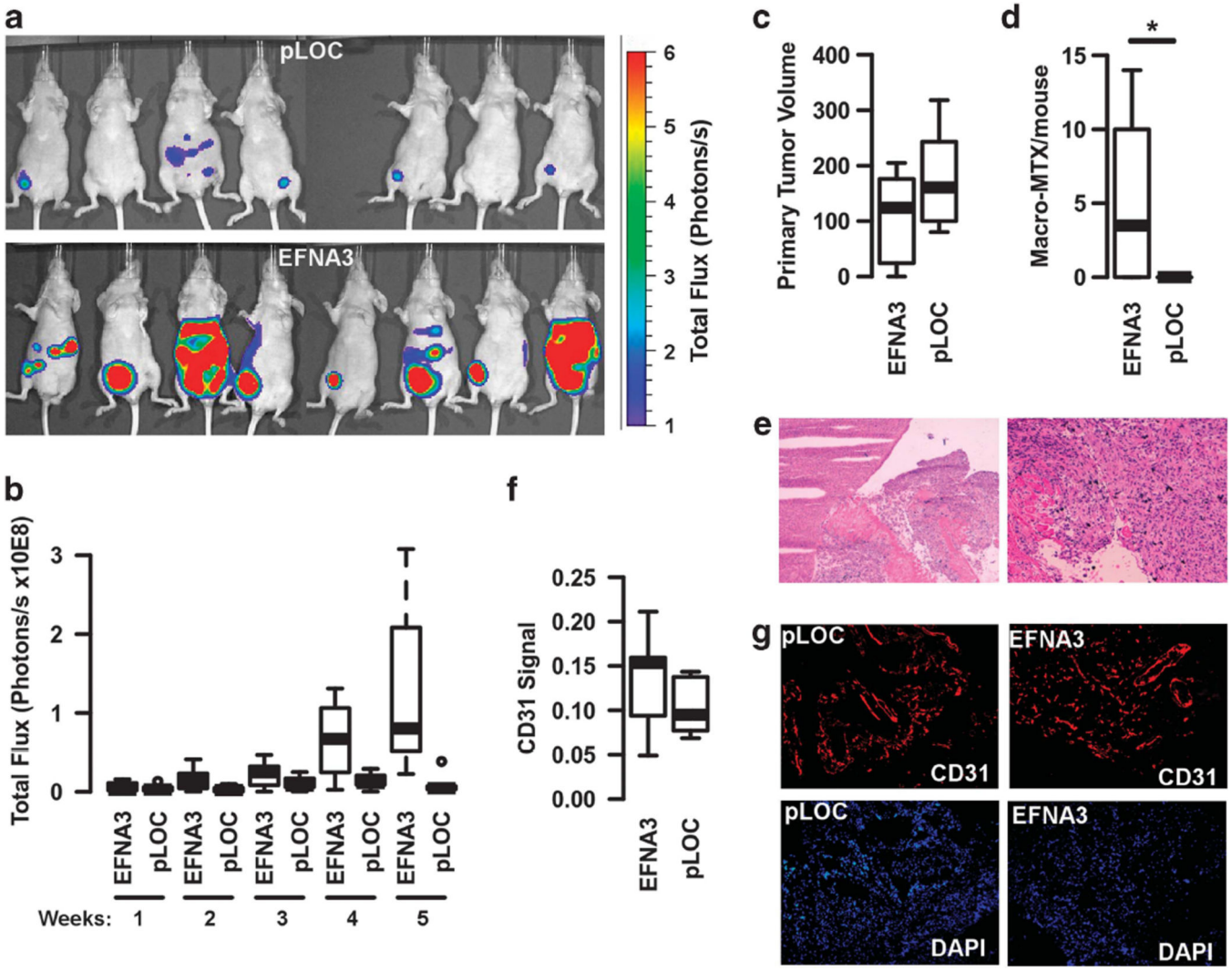

Figure 5.

EFNA3 overexpression increases metastasis formation in a spontaneous metastasis assay. MDA-MB-231 cells were engineered to stably express luciferase alone (pLOC) or in combination with *EFNA3* (*EFNA3*). Then, cells were orthotopically injected into the mammary fat pad of nude mice and tumor growth followed by noninvasive whole-body bioluminescence imaging (BLI). (**a**) BLI image of mice at end time point (5 weeks). (**b**) Luminiscence signal during the course of the experiment. The graph represents the luciferase signal (total flux) in photons per s $\times 10^8$. (**c**) Tumor volume was determined at 5 weeks. The boxplot represents the distribution of volume in each group. The differences between controls and *EFNA3*-expressing tumors was not significant (independent samples *t*-test: $t_{12} = -1.5373$, $P = 0.1499$). Animals were euthanized and tissues processed for hematoxylin and eosin (H&E) staining (**e**) or immunostaining (**f** and **g**). (**d**) The box-and-whisker plot represents the distribution of the number of macroscopic metastasis per mice identified by visual inspection during necropsy. The difference between groups was statistically significant (independent samples *t*-test: $t_7 = 2.5923$, $P < 0.05$). (**e**) Representative H&E staining images at × 10 (left) and × 40 (right) magnification. (**f**) Blood

vessels were stained with an antibody against human CD31 and cell nuclei with 4’,6-diamidino-2-phenylindole (DAPI). The CD31 signal was normalized to cellularity (DAPI staining). The graph represents the distribution of normalized values. Differences between groups were not significant (independent samples *t*-test: $t_{10} = 1.0522$, $P = 0.3182$). (**g**) Representative images of CD31 and DAPI staining.

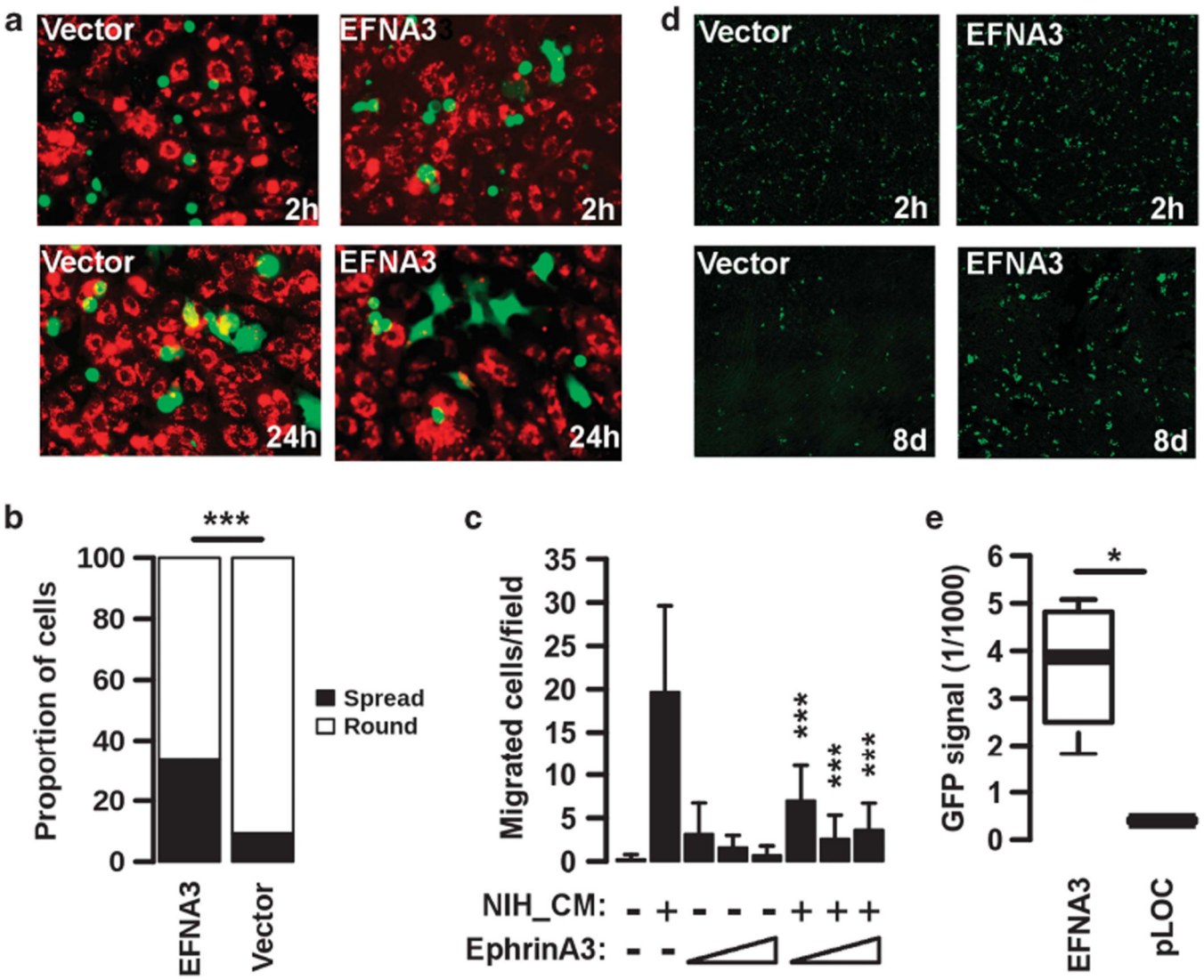

Figure 6.

EFNA3 expression results in repulsion of HUVEC cells and promotes extravasation. (**a** and **b**) HEK293T cells were transiently transfected with plasmids encoding for GFP and *EFNA3* (‘*EFNA3*’) or GFP alone (‘Vector’) and then plated on top of a monolayer of HUVEC previously labeled with a red fluorochrome. (**a**) Representative images of cells 2 and 24 h after plating HEK293T cells on top of the HUVEC monolayer. (**b**) The graph represents the proportion of GFP-positive cells attached to the plastic surface and spreading at 24h. The differences between cells expressing *EFNA3* and cells transfected with GFP alone was statistically significant (2 × 2 contingency table: χ^2_1=67.52, $P < 0.001$). (**c**) HUVEC migration was determined using NIH conditioned media (NIH_CM) as chemoattractant in the absence or presence of 0.2, 1 or 5 μg/ml of recombinant Ephrin-A3 fused to the Fc region of immunoglobulins (EphrA3). The graph represents the average number of migrated cells per field in a single experiment and error bars the s.d. The experiment was repeated three independent times with similar results. The differences among treatments was statistically significant (analysis of variance (ANOVA) $F_{7,178} = 47.17$, $P < 0.001$) and the

asterisks indicate means that were statistically significant to the NIH-conditioned media treatment (***adjusted $P < 0.001$) in a posteriori Tukey's test. (**d** and **e**) MDA-MB-231 cells stably expressing GFP alone or in combination with *EFNA3* were injected in the tail of nude mice. After the indicated periods of time, mice were euthanized and lungs were examined by confocal microscopy for the presence of GFP-positive cells. The boxplot represents the distribution of total GFP signal normalized to lung area in each group of mice. Results from two independent experiments were pooled. The differences between the two groups was statistically significant (Student's *t*-test $t(3) = -4.44$, $P < 0.05$).

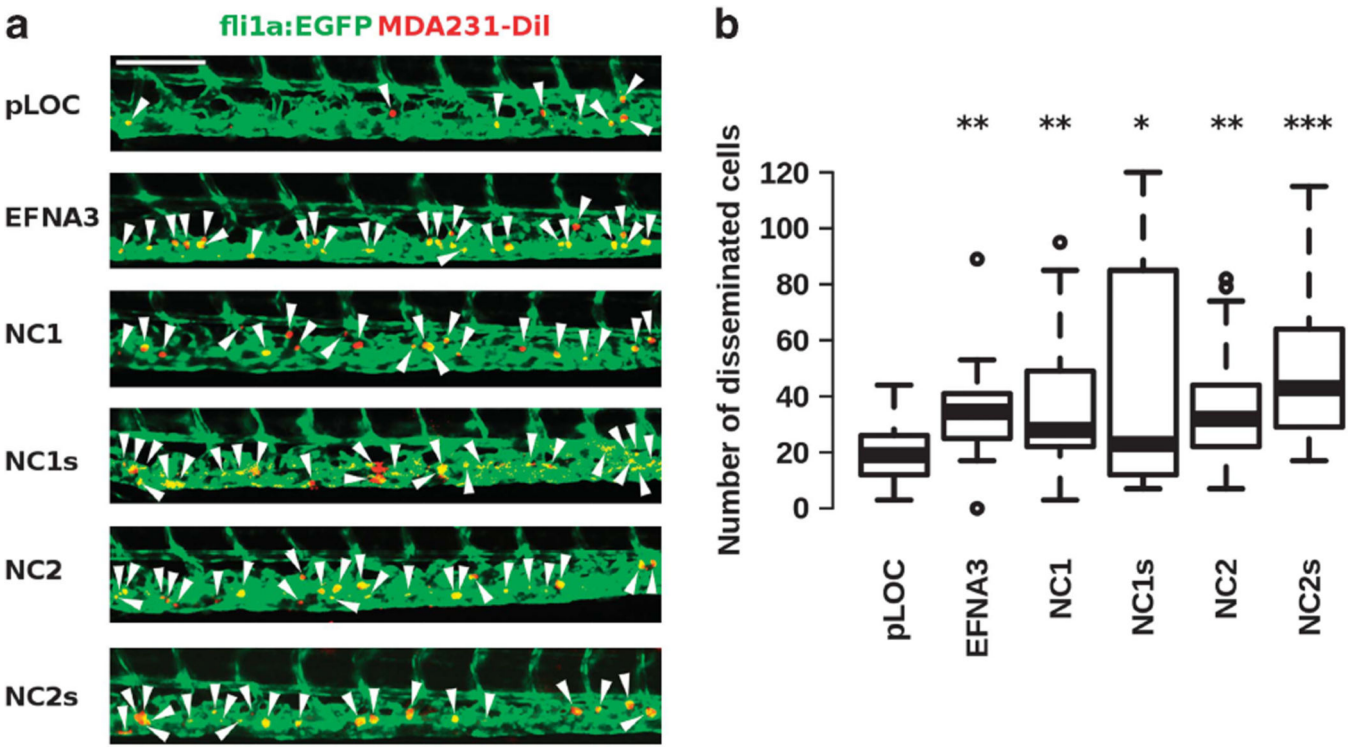

Figure 7.

Systemic dissemination of MDA-MB-231 cells is enhanced by the expression of *EFNA3*, NC1, NC2s, NC2 or NC2s. MDA-MB-231 cells infected at a multiplicity of infection (MOI) of 4 with lentivirus designed to induce expression of *EFNA3*, NC1, NC1s, NC2, NC2s or empty control (pLOC) and labeled *in vitro* with DiI dye. Then, approximately 100–500 cells were injected per embryo in the perivitelline space of 2-day-old transgenic Tg(fli1a:EGFP) zebrafish embryos. (**a**) Flourescent micrographs of the posterior tail showing distal dissemination of tumor cells (red) and their close association with the blood vessels of the embryo (green) 3 days after tumor cell implantation. Scale bar indicates 100 μm. White arrowheads indicate disseminated tumor cells. (**b**) The boxplots represent the number of distally disseminated tumor cells per fish (n = 17–41 fish per condition), 3 days after tumor cell implantation in the tail region. The differences between groups were statistically significant (analysis of variance (ANOVA) $F_{5,162} = 4.1$, $P < 0.01$) and the asterisks indicate means pairs that were the statistically significant (*$P < 0.05$, **$P < 0.01$, ***$P < 0.001$) in *a* posteriori pairwise *t*-test adjusted for multiple testing (Bonferroni).

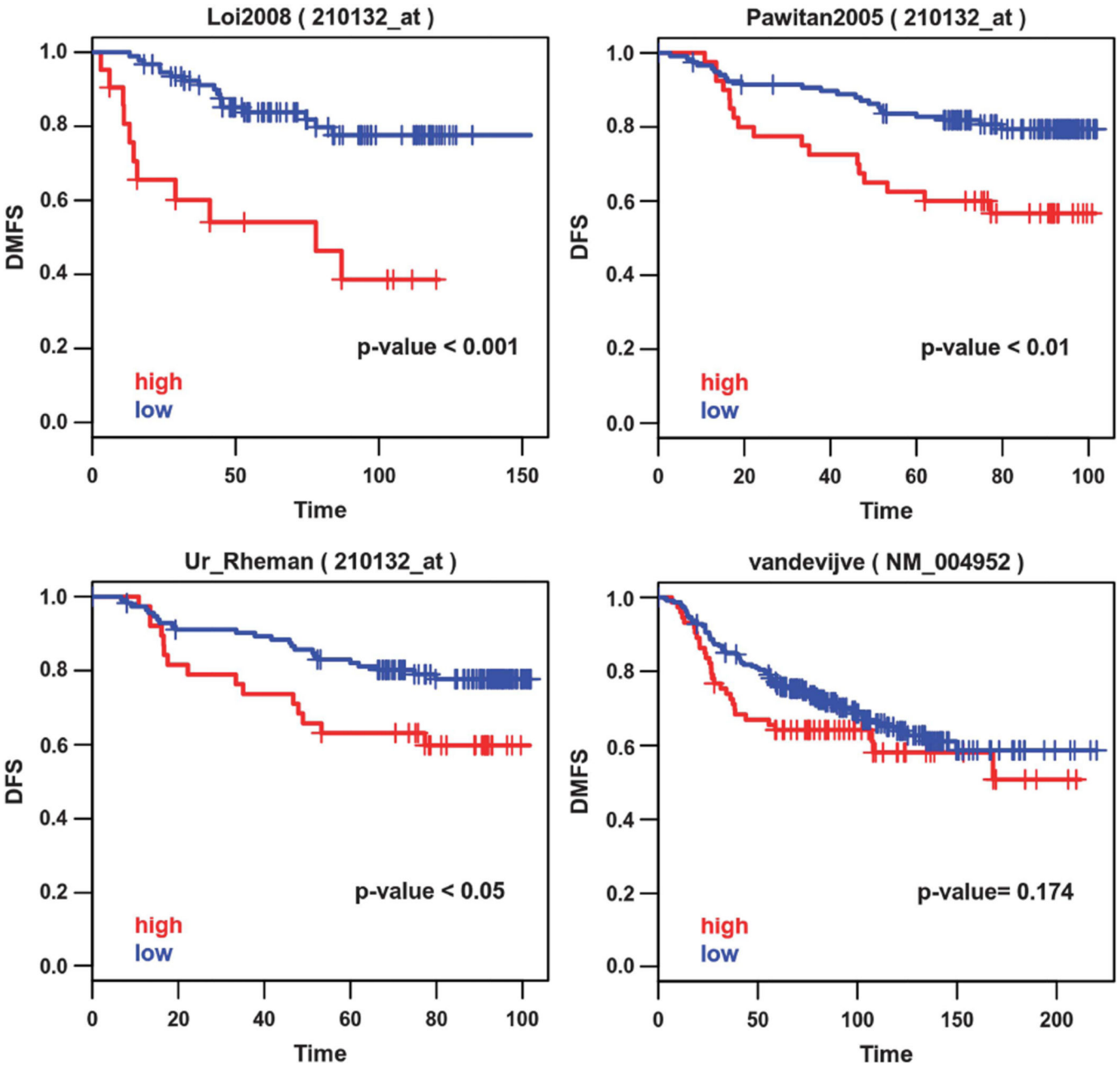

Figure 8.

High levels of *EFNA3* correlate with metastasis in human tumors. Gene expression profiles from the indicated series of breast cancer tumors (refs 51–53; Ur-Rehman, www.rock.icr.ac.uk/) were downloaded from the ROCK database (www.rock.icr.ac.uk/). Samples were categorized according to *EFNA3* expression into high (samples with *EFNA3* expression in the top quartile of the series, labeled in red) and low expression (rest of samples in the series, labeled in blue) and the Kaplan - Meier estimate of the distant metastasis-free survival (DMFS) over time calculated (graphs). The survival of the two groups was compared using a Cox proportional hazards model; the *P*-values are indicated in

the graphs. The probes used in the gene profiling assays are indicated within parentheses in the graph title.